Quinoxaline based nanoprobe for selective detection of Adenine in aqueous medium: Application to Biological sample

S. B. Suryawanshi[1], G. R. Deshmukh[2], A.J. Bodake[3]* and S. R. Patil[1]*
[1] Assistant Professor, [2]Research fellow, [3]Associate Professor
[1]Professor
[1]Department of Chemistry,
[1]Sanjay Ghodawat University, Kolhapur-416118, Maharashtra, (India).
[2]National Chemical Laboratory (NCL), Pune-411008, Maharashtra, (India).
[3]Rajaram College Kolhapur-416004.

Abstract: Quinoxaline based derivative 2,3-diphenyl quinoxaline (DPQ) was synthesized followed by spectral characterization. The aqueous suspension of DPQ nanoparticles (DPQNPs) were prepared by reprecipitation method. The average particle size of NPs obtained from Dynamic Light Scattering (DLS) examination is 52 nm. While field emission scanning electron microscopy (FE-SEM) analysis of air-dried film of aqueous suspension of NPs showed spherical morphology. Aggregation Induced Enhanced Emission (AIEE) of suspension of DPQNPs found red shifted when compared with emission arising from DPQ in THF solution. The zeta potential value of NPs is -23.3 mV indicates stability and ability of DPQNPs to interact with oppositely charged analyte molecules. The recognition test based on fluorescence shows quenching of fluorescence arising from DPQNPs suspension by addition of adenine (AD) solution. Effect of interfering substances on quenching capacity of adenine examined in presence of other ions indicated that adenine response is of high order while other ions responded negligibly. The possible mechanism of fluorescence quenching of NPs upon interaction with Adenine molecule was discussed on the basis of surface adsorption and ground state complex formation between them through H-bonding. Further the proposed fluorescence quenching method was successfully applied for the detection of adenine in serum sample by standard addition method.

1. INTRODUCTION

Design and synthesis of fluorescent nanosensors for the determination of chemically and biologically significant analyte is an active area of research [1]. Adenine is an important constituent of DNA which play a vital role in many biological systems [2]. It controls blood flow in human body, prevents cardiac arrhythmias, inhibits a neurotransmitter release and affects cerebral circulation [3, 4]. The unusual changes of adenine concentration in human body may lead to various diseases such as cancer, AIDS and myocardial cellular energy status [5, 6]. Hence the development of low-cost and selective method for the detection of adenine in the chemical, biological, clinical and medicinal sample is of current need. The existing techniques used for the detection of adenine are High Performance Liquid Chromatography (HPLC) [7], Surface Enhanced Raman Spectroscopy [8], Mass Spectrometry (MS) [9], Capillary electrophoresis [10], Flow Injection Chemiluminescence [11] and Fluorescence [12]. Though these conventional techniques have lower value of limit of detection (LOD), some of them suffers from the disadvantages like high cost, longer time and complicated pretreatment. In contrast fluorometric method has good sensitivity and selectivity towards determination of biologically important analyte molecules. Now a day's use of nanomaterials for the detection of biomolecules has given new sensor strategies [1]. Fluorescent organic nanoparticles (FONPs) have attracted enormous interest in the past few years due to their stability and reproducibility [13, 14]. Functionalized organic nanoparticles show strong AIEE and are extensively used as sensor materials in aqueous medium [15, 16]. Quinoxaline is an important class of nitrogen containing benzo heterocyclic compound [17, 18]. Presence of N-hetero atom in the ring may be effective to produce interaction with analyte species like adenine having H-donor ability to form complex [19-21]. O-Phenylenediamine is strongly fluorescent in organic solvents because of its better solubility. However, the solubility in water restricts its use for the preparation of NPs by reprecipitation method. The reprecipitation method requires highly hydrophobic fluorescent organic molecules. O-Phenylenediamine is known to undergo condensation with diketones. Use of aromatic diketones may yield the more conjugated and more hydrophobic molecules. With this idea in mind we proposed to prepare 2, 3-diphenylquinoxaline (DPQ) which could be more hydrophobic [22]. The nanoparticles of DPQ found highly fluorescent and the non-bonded electrons on N atom creating negative surface charge over the NPs may attract positively charged analyte species of importance. The recognition tests performed using different positively charged analyte species indicate that the fluorescence intensity of NPs of DPQ was strongly quenched only by the adenine. Thus, the method is developed for the sensing and detection of adenine in the aqueous solution using DPQNPs as a fluorescent probe. Further the developed quinoxaline based novel nanosensor system is successfully applied for the detection and quantification of adenine in serum samples using fluorescence quenching approach.

2. EXPERIMENTAL

2.1Material

Benzil (98%), O-Phenylenediamine (98.0%) and p-Toluene sulfonic acid (p-TSA) (98%) were procured from Sigma Aldrich (India) and Lobachem (Mumbai, India). Analytical grade ethanol (99%) and tetrahydrofurane (THF) (99.5%) were procured from Changshu Yangyuan Chemical (China) and Finar Chemicals Limited (Ahmadabad India) respectively. Adenine (AD) (99.0%) was purchased from HiMedia laboratories Pvt. Ltd Mumbai (India). Ultrapure water was used for the preparation of solutions in all experiments.

2.2 Synthesis of 2, 3-Diphenylquinoxaline (DPQ)

O-Phenylenediamine (0.108g, 1mmol), Benzil (0.210, 1mmol) and p-TSA (0.034 g, 2 mmol) were taken in flat bottom flask, dissolved in ethanol (5 mL). The reaction mixture was stirred for 10 minutes. The progress of reaction was monitored by thin layer chromatography (TLC) using ethyl acetate-pet ether (3:7) as solvent system. After completion of reaction, the content was poured on crushed ice and stirred again for 10 minutes. The solid separated was filtered, washed with water, dried in oven and crystallized in ethanol [23]. The synthesis route of DPQ is shown in Scheme 1.

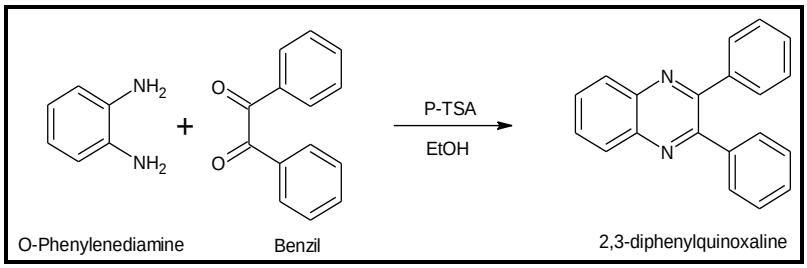

Scheme 1 Synthesis of 2, 3-diphenylquinoxaline (DPQ).

Spectral data for DPQ:

DPQ was obtained as white solid, 93 % yield, melting point 126ºC (literature 125-127 ºC), IR (Supplementary Figure S1) (cm^{-1}) 1659.45, 1599.66, 1441.19, 1313.29, 1213.31, 1175.4 due to C-C stretching of aromatic ring, 1213.31 cm^{-1} due to C-H in phenyl ring, The strong absorption band at 761.74 and 696.21 cm^{-1} indicates monosubstituted benzene ring, weak absorption band at 1441.53 cm^{-1} reveals –C=N stretching. ^{1}H NMR (300MHz, $CDCl_3$, δ ppm): (Supplementary Figure S2) 7.38 (dd, *J* = 6.9 Hz and 10.8 Hz, 6H), 7.52-7.56 (m, 4H), 7.78-7.82 (m, 2H), 8.20 (dd, *J* = 6.3Hz and 3.6 Hz, 2H).^{13}C NMR (75MHz, $CDCl_3$, δ ppm): (Supplementary Figure S3) 128.2, 128.8, 129.2, 129.8, 129.9, 139.1, 141.2, 153.4.

2.3 Preparation of nanoparticles of DPQ in aqueous suspension

2, 3-Diphenylquinoxaline nanoparticles were prepared by reprecipitation method developed in the laboratory using reported procedure [24, 25]. 2mL THF solution of DPQ (1×10^{-5}M) was rapidly injected through microsyringe into 100 ml aqueous solution at room temperature with vigorous stirring for 1 hour and further sonicated for 30 minutes in sonicator (Model UCB 40) to disperse the nanoparticles in water.

2.4 Characterization Techniques

FT-IR spectrum of DPQ was recorded on ATR PRO ONE Single-reflection (Model-FT/IR-4600 type A), Nuclear magnetic resonance (NMR) spectrum was recorded in deuterated chloroform ($CDCl_3$) on Bruker AC-300 NMR spectrometer (300 MHz for ^{1}H NMR and 75 MHz for ^{13}C NMR). Chemical shifts are reported using tetramethylsilane (TMS) as an internal standard. The particle size distribution and zeta potential of DPQNPs in aqueous suspension were measured using a Malvern Zetasizer (Nano ZS-90, U.K) equipped with 4MW, 633 nm, He-Ne Laser at 25 °C under fixed angle of 90° in disposable polystyrene cuvettes. A Field Emission Scanning Electron Microscope (FE-SEM, FEI Quanta 650 F) was used to examine the morphology of DPQNPs. UV-vis absorption spectra were recorded by using (Specord 210 plus) Analytical Jena using 1 cm quartz cell. A steady-state fluorescence spectrum of aqueous suspension of DPQNPs was recorded on Spectrofluorimeter (JASCO, Model FP-8300, Japan). The excitation and emission slits were fixed at 5 nm. The fluorescence life time was measured under conditions ($\lambda_{ex}/\lambda_{em}$= 246 nm/ 424 nm) using a Time-Correlated Single Photon Counting [TCSPC] spectrometer (HORIBA Jobin Yvon IBH) Japan.

3. RESULTS AND DISCUSSION

3.1 Particle size and morphology studies of DPQNPs

Figure 1a) shows the particle size distribution histogram of DPQNPs recorded by using dynamic light scattering (DLS) technique. The histogram shows that the particle size distribution is narrower in the range 30-100 nm and the average particle size is 52 nm. Further the FESEM image of airdried layer of suspension of NPs on silicon substrate shown in Figure 1 b) reveals spherical morphology. The average particle size of DPQNPs 110 nm obtained from FESEM is larger as compared to DLS exploration, owing to agglomeration of NPs occurred when water from suspension evaporated during formation of film on silicon substrate.

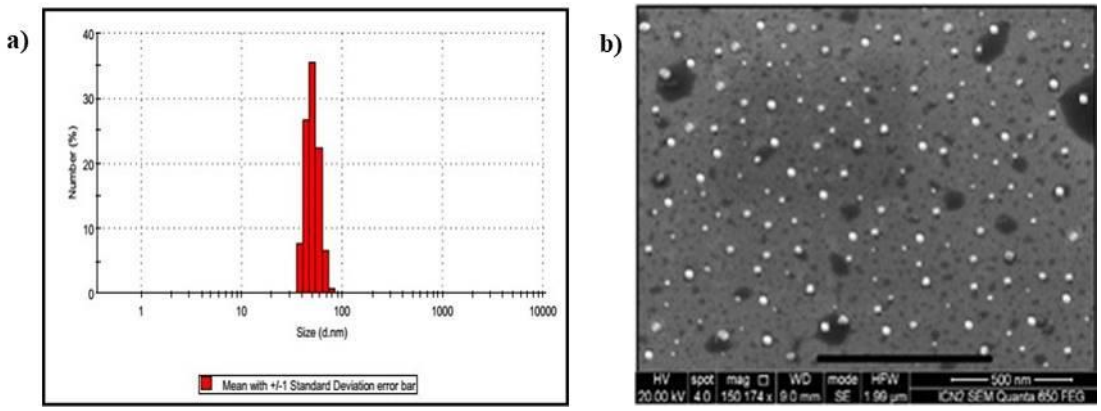

Fig. 1a) Particle Size Distribution histogram of DPQNPs obtained by DLS analysis. b) FE-SEM image of air-dried layer of aqueous suspension of DPQNPs.

3.2 Photophysical study of DPQNPs

3.2.1 UV-visible spectroscopy

Figure 2a) presents the absorption spectrum of aqueous suspension of DPQNPs (B) at pH=7 and absorption spectrum of dilute solution of DPQ sample molecule in THF (A). The absorption spectrum in UV region <300 nm of DPQ in THF shows strong absorption band attributed to aromaticity of the compound in addition to molecular absorption band seen in 300 to 375 nm with maximum at 347 nm owing to n → π* transitions. However, in the absorption spectrum of aqueous suspension of DPQNPs the band of n → π* disappears due to aggregation of molecules which prevent molecular transitions and blue shifted band of aggregate is seen at ≅ 246 nm. The blue shifted absorption band of NPs indicates H-type of aggregation due to lateral π-stacking interaction between neighbouring molecules which then forms spherical nanoparticles [26].

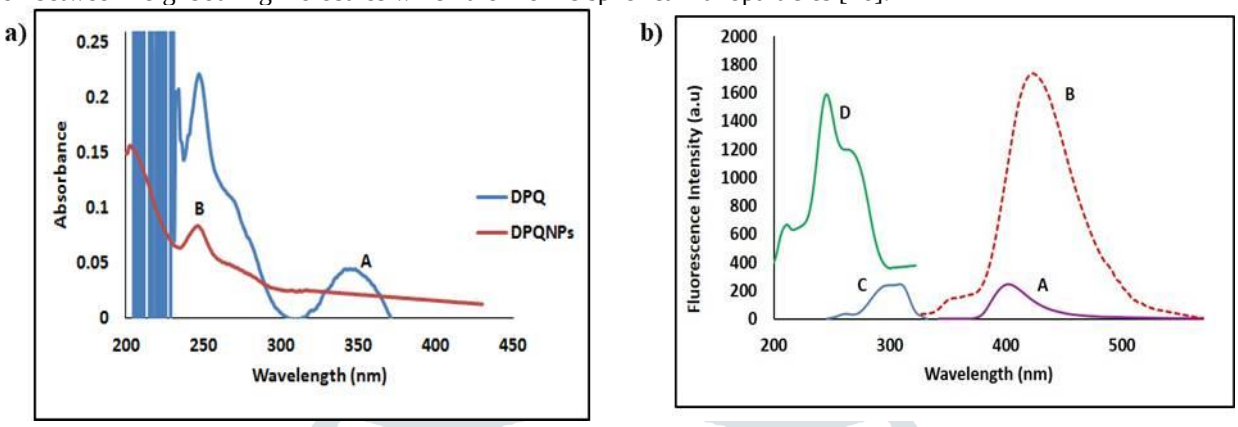

Fig. 2a) UV-visible absorption spectra of DPQ in THF solution (A) and DPQNPs in aqueous suspension (B) (at pH=7 using Phosphate buffer), **b)** Fluorescence emission (A) and excitation (C) spectra of DPQ in THF (1×10^{-5}M) and fluorescence emission (B) and excitation (D) spectra of aqueous suspension of DPQNPs (at pH=7, λ_{ex}= 246 nm).

Aggregation Induced Enhanced Emission (AIEE) of DPQNPs

The excitation spectrum of nanoparticles (D) is a structured b and peaking at 246 nm, whereas the excitation spectrum of DPQ in acetone (C) is peaking at 312 nm. The excitation spectrum of NPs is shifted towards lower wavelength with respect to excitation spectrum of DPQ momomer. The fluorescence spectrum (B) of nanoparticles (at pH=7) shown in Figure 2b) is a broad structureless band with maximum at 424 nm (monitored at excitation wavelength λ_{ex}= 246 nm). In contrast the fluorescence of DPQ in THF solution (A) peaking at 406 nm is a weak band arising from isolated molecules. The fluorescence of DPQNPs is red shifted from the molecular fluorescence of dilute solution of DPQ. The red shifted emission suggests the strong intermolecular attraction between neighbouring molecules, which resulted into aggregated nanoparticles. The aggregation in the form of nanosize restricts molecular rotation and vibration thus preventing nonradiative decay pathways of energy. The intensity of fluorescence at λ_{em}= 424 nm of nanoparticles is significantly stronger than the emission intensity of 1×10^{-5} M solution of DPQ from which nanoparticles are prepared. Such fluorescence emission observed from DPQNPs is the AIEE.

3.2.4 Recognition studies of Adenine (AD) using DPQNPs

The interaction of nanoparticles with different analyte molecular ions and metal ions were examined from fluorescence spectra of nanoparticles shown in Figure 3a. It is seen that the intensity of fluorescence at λ_{em}= 424 nm is drastically quenched by AD only, while others such as D-penicilliamine, Guanine, Erythromycine, Cyanocobalmine, Nicotinamide, Insitol, Thymine, 5-FU, L-Histadine, BSA, HSA and metal ions Cu^{2+}, Pb^{2+}, Zn^{2+}, Co^{2+}, Cd^{2+} and Fe^{2+} decreases the fluorescence negligibly. This observation indicates that DPQNPs can be used as a probe for selective sensing of AD in aqueous solution even in presence of other co-existing ions. The selectivity of nanoparticles is investigated from fluorescence decrease produced by AD in presence of 10 µM solution of each coexisting substances. The effect of fluorescence change estimated as $\frac{\Delta F}{F}$ is presented by the bar diagram in Figure S4, where ΔF is the difference in fluorescence intensity of nanoparticles without and with AD and other coexisting ions. The blue bar in Figure S4 shows selective sensing ability of DPQNPs towards AD only whereas, the remaining coexisting substances shows negligible response. The red bar seen in same figure reveals the fluorescence quenching of DPQNPs caused by AD is not affected even in presence of coexisting substances. This observation is in harmony with very negligible interference of coexisting species.

3.2.5 Fluorimetric titration of DPQNPs with AD solution

The fluorimetric titration was carried out by adding increasing amount of AD solution in the concentration range from 1 to 10 µM into the aqueous suspension of DPQNPs maintained at pH = 7.0. Fluorescence spectra shown in Figure 3b) reveal that as concentration of AD increases the emission intensity of NPs noted at maximum emission wavelength 424 nm decreases gradually. The increase in concentration does not affect spectral energy distribution of NPs.

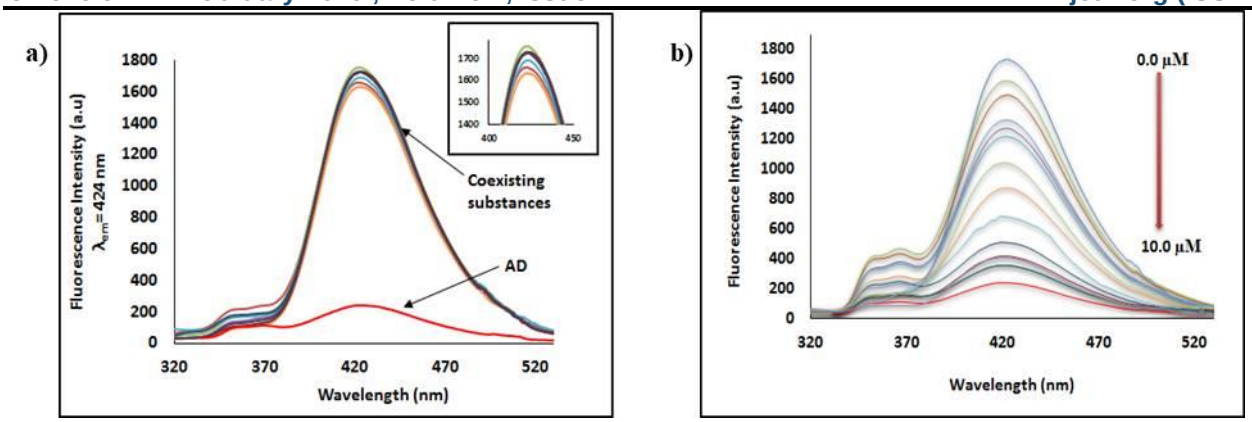

Fig. 3a) Fluorescence spectra of aqueous suspension of DPQNPs in presence of various coexisting substances 10 µM each concentration, at λ_{ex}= 246 nm, **b)** Fluorescence spectra of DPQNPs suspension in presence of AD of concentration 0.0, 1.0, 2.0, 3.0, 3.5, 4.0, 5.0, 6, 7.0, 8.0, 8.5, 9.0, 10 µM.

3.2.6 Statistical analysis and Detection Limit

The quenching results found to fit into conventional Stern-Volmer relation. The plot of $\frac{F_0}{F}$ versus concentration of AD solution shown in Figure 4a) is linear in the concentration range from 0.0 µM to 7 µM with intercept value on Y-axis equal to one.

$$\frac{F_0}{F} = 1 + K_{SV}[Q] = 1 + k_q \tau_0 [Q] \quad (2)$$

where F_0 and F are the fluorescence intensities of the DPQNPs without and with AD of different concentrations, K_{SV} is the Stern–Volmer quenching constant (K_{SV} = 1.702 ×10^5 M^{-1}), [Q] is the concentration of the AD solution and k_q is the quenching rate constant (k_q= 1.356 ×10^{14} M^{-1} Sec^{-1}), τ_0 is the fluorescence lifetime of NPs in absence of quencher. The correlation coefficient obtained from plot R^2= 0.9901 indicates linear fit of quenching data. However, the plot of $\frac{\tau_0}{\tau}$ *Vs* concentration of AD shown in Figure 4a) is straight line parallel to x-axis because the fluorescence life time is independent of concentration of fluorophore. Such observations are in harmony of the static quenching type of fluorescence quenching of NPs [27].
The limit of detection (LOD) was calculated by using an equation (3).

$$LOD = \frac{3.3\sigma}{k} \quad (3)$$

where 'σ' is the standard deviation of y intercept of the regression line and 'k' is the slope of the calibration graph. The limit of detection (LOD) of the proposed fluorescence method is 0.7061 µM.

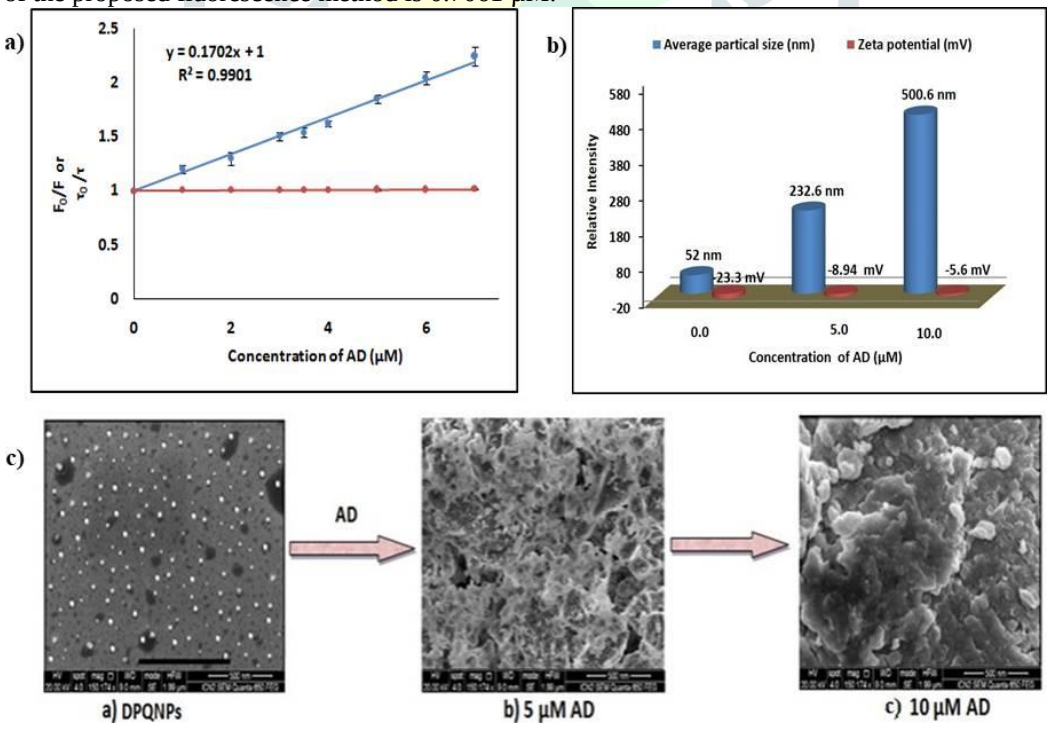

Fig. 4a) Comparative Stern–Volmer plot of F_0/F or τ_0/τ verses addition of different amounts of the Adenine solution (0.0, 1.0, 2.0, 3.0, 3.5, 4.0, 5.0, 6, 7.0µM), b) Bar diagram showing effect of AD concentration on particle size and zeta potential of DPQNPs. c) FE-SEM image of airdried film of aqueous suspension of DPQNPs with increase in concentration of AD 5µM and 10 µM respectively.

3.2.7 Mechanism of fluorescence quenching of aqueous suspension of DPQNPs by AD

The possible mechanism of fluorescence quenching of NPs upon interaction with AD molecule was discussed on the basis of the surface adsorption and ground state complex formation between them through H-bonding. The surface adsorption and binding interaction between NPs-AD complex was discussed with the assist of zeta potential values, FE-SEM analysis and double logarithmic plot. The Figure 4b) shows the bar diagram of variation of zeta potential and size of NPs in the absence and presence of AD solution. The initial size 52 nm of the NPs without AD found to be increased to 232.6 nm and 500.6 nm on addition of 5 µM and 10 µM AD solution respectively. Similarly, the zeta potential shown in same figure decreased from -23.3 mV to -8.94 and -5.6 mV on addition of 5 µM and 10 µM of AD respectively. The decrease in zeta potential value and increase in particle size suggests the possibility of adsorption of AD on the negatively charged surface of NPs. To support this surface adsorption the FE-SEM analysis was taken. Figure 4c) presents the FE-SEM images of air-dried films of aqueous suspension of NPs (a) without and with 5µM and 10 µM AD solution respectively (b & c). It is seen that the spherical morphology of DPQNPs deformed to flow like structure due to destabilization of NPs upon adsorption of AD on the surface.

The binding constant 'K' and binding sites 'n' obtained from the double logarithmic plot by using following equation (4) [28].

$$Log_{10}\frac{(F_0-F)}{F} = Log_{10}K + nLog_{10}[AD] \quad (4)$$

where, F_0 and F are the fluorescence intensities of NPs in absence and presence of AD concentration. The values of 'K' and 'n' for NPs-AD complex were determined by double logarithmic plot $Log\frac{(F_0-F)}{F}$ Vs Log $[AD]$ shown in Figure S5. The value of K obtained from the plot is 3.482×10^2 Lit. mol^{-1} which indicates good stability of NPs-AD complex at room temperature. The value of binding sites from the plot is 1.9889 which is approximated to nearest integer 2, indicates two possible binding sites available on the surface of NPs. AD interacts with NPs through hydrogen bond with co-ordinating N atom in phenyl ring of quinoxaline as presented in Scheme 2. Water molecules are also competing to undergo hydration through hydrogen bonding. However, the hydrophobic interactions between DPQ molecules forming nanoaggregates are protected from solvent hydration and hydrogen bonding between DPQNPs and adenine is strengthened. The observed decrease in zeta potential of aqueous suspension of DPQNPs with addition of AD led us to consider that, out of the two hydrogen atoms of amino group of AD, one engage in hydrogen bonding through N atom in DPQNPs while other involve in hydration with water. So also the remaining N atom of AD undergoes hydration with water as shown in the proposed scheme of interaction (Scheme 2), which is the reason of observed quenching of fluorescence intensity of DPQNPs in aqueous suspension.

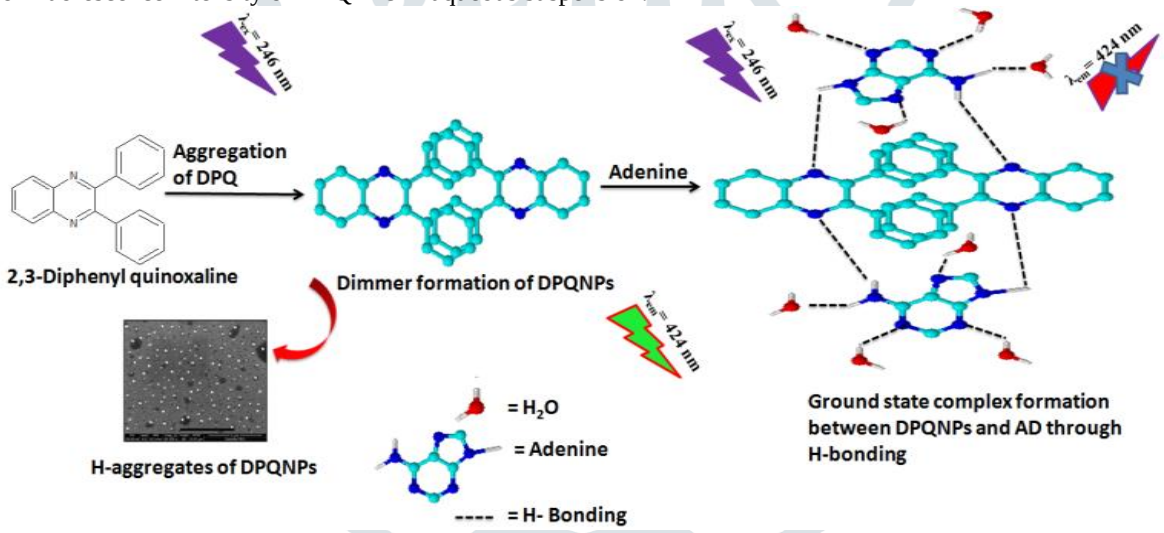

Scheme 2 Schematic representation of interaction and ground state complex formation between AD and DPQNPs through hydrogen bonding.

3.2.8 Application of the proposed scheme for the detection of AD in Biological sample

The practical applicability of the proposed method was explored for the analysis of biological sample (serum sample) obtained from nearby university campus. An appropriate amount of the serum sample was diluted prior to use. The serum samples were spiked with AD to prepare synthetic samples of concentration 3µM and 7µM, and diluted within working range by distilled water and analysed fluorimetrically using standard addition method.

Table 1 Analysis of Serum sample for AD content using Standard addition method.

Samples	Amount of AD added (µM)	Amount of AD Found (µM)	RSD (n=3) %	Recovery %
Serum 1	3.0	2.963	1.069	98.75
Serum 2	7.0	6.956	1.057	99.37

The results obtained from the calibration graph given in Figure 4a) are shown in Table 1. The close agreement within experimental values between the AD added and found indicates the reliability of the proposed method for quantification of AD using aqueous suspension of DPQNPs as fluorescent probe.

4. Conclusion

The small molecular weight fluorescent organic molecule was designed, using O-Phenylenediamine as parent molecule. The condensation of O- Phenylenediamine with Benzil has given fluorescent 2, 3- Diphenylquinoxaline molecule. The nanoparticles of DPQ was prepared by using reprecipitation method exhibits strong red shifted fluorescence owing to AIEE as compared to fluorescence of sample molecule arising from isolated molecules in dilute THF. The NPs are found to be spherical with average particle size of 52 nm. The fluorescence of DPQNPs suspension is found to be quenched selectively by adenine only even in presence of the other coexisting substances which does not affected the fluorescence of NPs. Thus, it is concluded that the DPQNPs selectively sense the adenine from biological sample.

Acknowledgements

The author SBS gratefully acknowledge the Department of Chemistry, School of Science, Sanjay Ghodawat University, Kolhapur and Department of Chemistry, Shivaji University Kolhapur for providing instrumental facilities procured through the support of Department of Science and Technology, Delhi and University Grants Commission (UGC), Delhi for providing funds to the Department of Chemistry under FIST and SAP-DRS phase-II programs.

References:

1. Devi, L. M. and Negi, D. P. S. 2011. Sensitive and selective detection of adenine using fluorescent ZnS nanoparticles. Nanotechnology, 22: 245502.
2. Heisler, I., Keller, J., Tauber, R., Sutherland, M. and Fuchs, H. 2002. A colorimetric assay for the quantitation of free adenine applied to determine the enzymatic activity of ribosome-inactivating proteins. Analytical Biochemistry, 302:114-122.
3. Li, S. P., Li, P., Dong, T. T. X. and Tsim, K. W. Determination of nucleosides in natural cordycepssinensis and cultured cordycepsmycelia by capillary electrophoresis, Electrophoresis, 22:144.
4. Malathi, R. and Johnson, I. M. 2001. From RNA World to Protein: An Eagle's eye view of the role of guanosine in tracing the antiquity of the intron. Journal of biomolecular Structure & Dynamics, 18:709.
5. Yang, F. Q., Guan, J. and Li, S. P. 2007. Fast simultaneous determination of 14 nucleosides and nucleobases in cultured cordyceps using ultra-performance liquid chromatography, Talanta, 73:269-273.
6. Duan, R., Li, C., Liu, S., Liu, Z., Li, Y., Yuan, Y. and Hu, X. 2016. Determination of adenine based on the fluorescence recovery of the L-Tryptophan-Cu^{2+} Complex. Spectrochimica Acta Part A: Molecular and Biomolecular Spectroscopy, 152:272–277.
7. Gill, B. D. and Indyk, H. E. 2007. Development and application of a liquid chromatographic method for analysis of nucleotides and nucleosides in milk and infant formulas. International Dairy Journal, 17:596.
8. Amri, C. E., Baron, M. H. and Maurel, M. H. X. 2003. Adenine and RNA in mineral samples. Surface enhanced raman spectroscopy (SERS) for picomole detections. Spectrochimica Acta Part A: Molecular and Biomolecular Spectroscopy, 59:2645.
9. Huang, Y. F. and Chang, H. T. 2007. Analysis of adenosine triphosphate and glutathione through gold nanoparticles assisted laser desorption/ionization mass spectrometry. Analytical Chemistry, 79:4852.
10. Yeh, C. F. and Jiang, S. J. 2002. Determination of monophosphate nucleotides by capillary electrophoresis inductively coupled plasma mass spectrometry. Analyst, 127:1324.
11. Liu, E. B. and Xue, B. C. 2006. Flow injection determination of adenine at trace level based on luminol- $K_2Cr_2O_7$ chemiluminescence in a micellar medium. Journal of Pharmaceutical and Biomedical Analysis, 41:649-653.
12. Ishikawa, M., Maruyama, Y., Ye, J. Y. and Futamata, M. 2002. Single-molecule imaging and spectroscopy of adenine and an analog of adenine using surface-enhanced raman scattering and fluorescence. Journal of Luminescence, 98:81-89.
13 Horn, D. and Rieger, J. 2001. Organic nanoparticles in the aqueous phase-theory experiments and use. Angewandte Chemie International Edition, 40:4330-4361.
14 Yasukuni, R., Asahi, T., Sugiyama, T., Masuhara, H., Sliwa, M., Hofkens, J., Schryver, F. C. D., Van der Auweraer, M., Herrmann, A. and Mullen, K. 2008. Fabrication of fluorescent nanoparticles of dendronized perylenediimide by laser ablation in water. Applied Physics A, 93:5–9.
15 Mahajan, P. G., Bhopate, D. P., Kolekar, G. B. and Patil, S. R. 2015. N-Methyl isatin nanoparticles as a novel probe for selective detection of Cd^{2+} ion in aqueous medium based on chelation enhanced fluorescence and application to environmental sample. Sensor and Actuators B: Chemical, 220:864–872.
16 Suryawanshi, S. B., Mahajan, P. G., Bhopate, D. P., Kolekar, G. B., Patil, S. R. and Bodake, A. J. 2016. Selective recognition of MnO_4^- ion in aqueous solution based on fluorescence enhancement by surfactant capped naphthalene nanoparticles: Application to ultratrace determination of $KMnO_4$ in treated drinking water. Journal of Photochemistry Photobiology A, 329:255-261.
17 Bharagava, D. and Garg, G. 2012. Recent trends in synthesis of quinoxaline and its derivatives. Journal of pharmaceutical research, 5(1):130-134.
18 Padvi, P. A., Mahale, G. H., Pawar, D. E., Falak, C. S. and Kendre A. V. 2015. Synthesis and biological activity of quinoxaline derivatives. World journal of pharmaceutical research, 4 [7]:1892-1900.
19 Cui, W., Wang, L., Xiang, G., Zhou, L., An, X. and Cao, D. 2015. A Colorimetric and fluorescence "Turn-Off" chemosensor for the detection of silver ion based on a conjugated polymer containing 2,3-di(pyridin-2-yl) quinoxaline. Sensor and Actuators B: Chemical, 207:281-290.
20 Yeh, C. W. and Ray, U. 2009. Syntheses, structures and luminescent properties of metal halide complexes containing 2, 3-diphenylquinoxaline. Journal of The Chinese Chemical Society, 56:1216-1224.
21 Zapata, F., Caballero, A., Molina, P. and Tarraga, A. 2010. A ferrocene-quinoxaline derivative as a highly selective probe for colorimetric and redox sensing of toxic mercury (II) cations. Sensor, 10:11311-11321.
22 Bendale, A. R., Kotak, D., Damahe, D. P., Narkhede, S. P., Jadhav, A. G. and Vidyasagar, G. 2011. Novel green approaches for synthesis of quinoxaline derivatives, Der Chemica Sinica, 2(2):20-24

23 Mahadik, P., Jagwani, D. and Joshi, R. 2014. A greener chemistry approach for synthesis of 2, 3 diphenylquinoxaline. International Journal of Innovative Science Engineering and Technology, 1 [6].

24 Kasai, H., Kamatani, H., Okada, S., Oikawa, H., Matsuda, H. and Nakanishi, H. 1996 Size dependent colors and luminescences of organic microcrystals. Japanese Journal of Applied Physics, 35: L221.

25 Kasai, H., Nalwa, H. S., Oikawa, H., Okada, S., Matsuda, H., Minami, N., Kakuta, A., Ono, K., Mukoh, A. and Nakanishi, H.1992. A Novel preparation method of organic microcrystals. Japanese Journal of Applied Physics, 31: L1132.

26 Lim, S., An, B., Jung, S., Chung, M. and Park, S. Y. 2004. Photoswitchable organic nanoparticles and a polymer film employing multifunctional molecules with enhanced fluorescence emission and bistable photochromism, Angewandte Chemie International Edition, 43:6346–6350.

27 Suryawanshi, S. B., Mahajan, P. G., Kolekar, G. B., Bodake, A. J. and Patil, S. R. 2019. Selective recognition of Cr(VI) ion as $Cr_2O_7^{2-}$ in aqueous medium using CTAB capped Anthracene based nanosensor: Application to environmental water sample. Journal of Physical Organic Chemistry, 32 (4):e3923.

28 Jiang, X. Y., Li, W. X. and Cao, H. 2008. Study of the interaction between trans-resveratrol and BSA by the multispectroscopic method. Journal of Solution Chemistry, 37:1609–1623.